



1 **Tangible and intangible ex-post assessment of flood-induced** 2 **damages to cultural heritage**

3 Claudia De Lucia, Michele Amaddii, Chiara Arrighi

4 Department of Civil and Environmental Engineering, Università degli Studi di Firenze, Via di S. Marta 3, 50139,
5 Florence, Italy

6 *Correspondence to:* Chiara Arrighi (chiara.arrighi@unifi.it)

7 **Abstract.** Floods pose significant risks to cultural heritage (CH), yet post-disaster damage data to CH remain lacking. In
8 this paper, we address this gap by focusing on the ex-post assessment of flood-induced damage to CH. The method
9 involves the identification of damaged assets, and a field survey to assess tangible (LTV) and intangible (LIV) damage.
10 The potential contributing factors e.g., water depth and river slope, are analyzed through geospatial analysis. Ex-post
11 damage data to CH are compared with the outcome of an ex-ante analysis based on available methods to verify the quality
12 of exposed data and possible limitations. The method is applied to the 15-16 September 2022 flood event that occurred
13 in the Marche Region (Italy). The survey involved 14 CH in 4 municipalities and 3 catchments. Results highlight the
14 inadequacy of existing exposure data for ex-ante damage assessment. However, ex-post data confirm that religious
15 architectures are likely to suffer the highest LTV and LIV. The ex-post damage analysis provided a semi-quantitative
16 evaluation of both LTV and LIV in relation to flood characteristics. Notably, significant correlations between LTV and
17 flood depth, as well as with the slope of the riverbed (a proxy for river flow velocity), were found. LIV correlates well to
18 flood depth and river slope although with lower R^2 and larger RMSE, highlighting that intangible impact analysis requires
19 more effort than hazard characterization. Further research should increase the availability of ex-post damage data to CH
20 to pose the basis for damage model validation and development of empirical vulnerability functions.

21 **1 Introduction**

22 Floods are among the most frequent and costliest natural hazards (CRED, 2015; Wallemacq et al., 2015). In recent
23 decades, the frequency and intensity of heavy rainfall, associated with ongoing climate change have consequently led to
24 an increase in flood events (Merz et al., 2021; IPCC, 2023). Moreover, due to severe urbanization and increasing
25 development in flood-prone areas, flood impacts are expected to grow in the future (Dottori et al., 2023).

26 The EU Flood Directive calls upon member countries to mitigate the potential adverse consequences of flooding on
27 human health, the environment, cultural heritage, and economic activities (EU Flood Directive, 2007/60/EC). Concerning
28 cultural heritage (CH), this purpose gains even more significance. Indeed, CH assets are severely affected by floods and
29 are likely to be increasingly threatened by climate change effects (Marzeion and Levermann, 2014; Fatoric and Seekamp,
30 2017; Sesana et al., 2021). In many cases, substantial costs for restoration are necessary, and in the worst-case scenario,
31 the irreversible destruction of unique and irreplaceable assets that hold cultural significance is unavoidable (Arrighi, 2021;
32 Arrighi et al., 2023b). Furthermore, the impact of floods on CH extends beyond the tangible damage, affecting social
33 identity and cohesion (Romão et al., 2020).

34 Cultural heritage can be defined as the legacy of tangible and intangible attributes inherited from past generations.
35 Tangible attributes include buildings, monuments, and historic places, as well as works of art, literature, music, and
36 artifacts both archaeological and historical. Intangible attributes comprise social customs, traditions, and practices, rooted
37 in aesthetic and spiritual beliefs and oral traditions (Willis, 2014).



38 Over the past decades, ex-ante damage assessment, namely impact analysis and mitigation measures of natural hazards
39 to CH assets, such as floods, received considerable scientific attention. Many researchers focused on individual assets or
40 site levels (Sabbioni et al., 2006; Drdácý, 2010; Huijbregts et al., 2014; Sesana et al., 2021; Momčilović Petronijević
41 and Petronijević, 2022; Anderson, 2023). Other studies focused on the negative effects of natural hazards on CH
42 concerning societal impacts and economic losses (Alexandrakis et al., 2019; Garrote et al., 2020). Additionally, several
43 studies have focused on flood risk assessment of CH at various scales, ranging from specific sites (Garrote et al., 2019;
44 Zhang et al., 2024), to cities (Wang, 2015; Arrighi et al., 2018; Trizio et al., 2021; Schlumberger et al., 2022; Arrighi et
45 al., 2023a; Brokerhof et al., 2023; Ravan et al., 2023), regions (Godfrey et al., 2015; Figueiredo et al., 2020; Arrighi et
46 al., 2023b), national levels (Stephenson and D'Ayala, 2014), and even globally (Reimann et al., 2018; Arrighi, 2021).
47 The ex-ante analyses represent a key aspect of any "flood risk management plan", as required by the EU Flood Directive
48 (EU Flood Directive, 2007/60/EC). However, estimating the loss after an event is equally important to support emergency
49 management and decide priorities for reconstruction and victim compensation (Molinari et al., 2014). Furthermore,
50 identifying key factors influencing the vulnerability of CH assets is necessary for a more robust risk assessment.
51 Achieving this requires the availability of post-disaster loss information and data, coupled with appropriate ex-post
52 damage analyses. Such endeavours would highlight weaknesses in current risk management practices and thus improve
53 the effectiveness of preparedness and resilience strategies (Arrighi et al., 2022). Nevertheless, there are only a few
54 examples in the literature concerning the ex-post assessment of damage to CH. In the work of Vecvagars (2006), an
55 overview of the different available methods in assessing the value of CH assets, providing some recommendations for
56 valuing damages and losses after a disaster, is outlined. Since 2008, the European Commission, the United Nations
57 Development Group, and the World Bank developed the joint Post-Disaster Needs Assessment (PDNA) tool. This tool
58 provides a comprehensive, government-led assessment of post-disaster damages, losses, and recovery needs, paving the
59 way for a consolidated recovery framework. The PDNA framework encompasses the gathering of data on damages to
60 both tangible and intangible values of cultural assets. More recently, a reviewed version of the PDNA, based on
61 experiences gathered through the analysis of many PDNA post-disaster assessments conducted since 2008, was published
62 (Jeggle and Boggero, 2018). Vafadari (2017) developed a tool for the recording and inventory of sites and monuments as
63 well as to record damage and threats, their causes, and assess their magnitude. Deschaux (2017) details the observed
64 impacts on movable and immovable heritage following the floods in Central France in 2016. Figueiredo et al. (2021)
65 analyze the impacts of wildfires that occurred in Portugal on cultural heritage integrating geospatial analysis with
66 information provided directly by municipalities affected by the wildfires.

67 As already mentioned, CH assets are characterized by both tangible and intangible value, and consequently, the damage
68 they suffer can be tangible and intangible. Therefore, for an adequate assessment of flood damage to CH, a classification
69 of these values is necessary (Romao et al., 2020), whether the analysis is conducted ex-ante or ex-post. Vecvagars (2006)
70 groups cultural heritage values into "use value" (related to market value) and "non-use value" (i.e., non-market value such
71 as spiritual value, legacy value, and social value). In addition, use value can be further divided into "extractive use value"
72 and "non-extractive use value". Extractive use value includes consumptive value, which can be measured through market
73 transactions. Non-extractive use value originates from the service the asset provides and includes aesthetic and
74 recreational values.

75 However, it is often noted that quantitative disaster data concerning losses related to cultural heritage are either scarce or
76 entirely unavailable (Romão et al., 2020). This underscores the persistent challenges in obtaining comprehensive
77 information on the impact of disasters on cultural heritage, emphasizing the need for improved data collection and
78 assessment methodologies in this critical domain, which are essential for damage model calibration and validation.



79 This paper focuses on the analysis of damage to CH assets as a consequence of a flood event. First, an ex-ante analysis
80 was performed using the available data. The official existing hydraulic hazard maps and the national CH database were
81 considered. However, the pivotal aspect of this study lies in the ex-post damage assessment. A well-defined workflow
82 has been proposed to assess the tangible and intangible losses incurred by CH due to flooding: (i) identification of the
83 assets potentially damaged by the flood; (ii) field data collection for the assessment of damage to CH; (iii) ex-post damage
84 assessment considering both tangible and intangible values of the damaged assets; (iv) analysis of the possible
85 contributing factor of the damage to CH.

86 The proposed method is applied to the case study of the flood event that interested the Marche Region (Central Italy) on
87 15-16 September 2022. The involved sites encompass different types of assets such as churches, historic bridges, and
88 industrial buildings, which are located in three basins in the Marche region: Burano, Cesano, and Misa.

89 Through the method proposed in this paper, we aim to fill the gap in the literature concerning ex-post assessment of
90 cultural heritage damage induced by floods. The research pinpoints the factors that significantly contribute to the
91 vulnerability of cultural heritage and the resulting flood-related damages.

92 **2 Materials and methods**

93 This section outlines the evaluation of flood damage to CH assets using two approaches: ex-ante and ex-post. Sect. 2.1
94 details the ex-ante damage analysis, which was conducted using available data. On the other hand, Sect. 2.2, the focus of
95 the paper, describes the procedure for the ex-post damage assessment.

96 **2.1 Ex-ante damage assessment**

97 The aim of the ex-ante damage assessment is to investigate if using the available data before the flood event, it would
98 have been possible to predict the degree of flood damage to CH. The database of CH considered for this analysis consists
99 of the assets included in the national MIC database (Istituto Superiore per la Conservazione ed il Restauro – MiBACT,
100 2024). The database contains movable and immovable assets under protection with declared cultural interest. In addition,
101 it includes assets older than 50 or 70 years under evaluation to verify their effective cultural interest (D.lgs. 22 gennaio
102 2004, n. 42). The assets that overlap with the official map of flood hazard areas are then considered. The ex-ante damage
103 assessment was evaluated as the combination of exposure and vulnerability (Arrighi et al., 2023b).

104 Exposure of CH can be evaluated by intersecting the shapefile of CH with the official flood hazard map available from
105 the website of the competent authority (AUBAC, 2024). As the MIC database does not provide information about the
106 value of the assets and only contains items of national listing, an exposure score equal to 1 ($E = 1$) is assigned to all
107 assets that overlay areas with some probability of inundation (i.e., P3 – high probability; P2 – medium probability; P1 –
108 low probability). On the other hand, a 0 score is attributed to all those assets that are not potentially flooded.

109 According to the vulnerability classification of Arrighi et al. (2023b), a vulnerability class is defined for each CH based
110 on its typology.

- 111 - Very high vulnerability: religious, residential, tertiary, fortified architectures, and museums.
- 112 - High vulnerability: industrial, productive, rural architectures, and monuments.
- 113 - Medium vulnerability: archaeological areas, infrastructure, and plants.
- 114 - Low vulnerability: open spaces.



115 According to this approach and based on the available data, considering the same value ($E=1$) for all assets then results
116 in damage equal to vulnerability.

117 **2.2 Ex-post damage assessment: The workflow**

118 The proposed workflow consists of 4 steps. The first step is focused on the identification of CH assets actually damaged
119 by the flood (Sect. 2.2.1). Then, in the second step, a post-event field survey, based on on-site visual inspection, is
120 conducted to evaluate the actual state and condition of CH assets (Sect. 2.2.2). Once all the data and information on the
121 damage to CH assets is obtained, the ex-post evaluation can be carried out assigning to the assets both tangible and
122 intangible values and related losses (Sect. 2.2.3). Lastly, the analysis of which factors contributed most to the damage, by
123 means of geospatial methods, is performed (Sect. 2.2.4).

124 **2.2.1 Identification of CH assets potentially damaged by the flood**

125 The initial step is dedicated to identifying CH assets situated within the flooded areas. The CH database of MIC could be
126 considered for this analysis. The data can be downloaded from the MIC cartographic tool (Istituto Superiore per la
127 Conservazione ed il Restauro – MiBACT, 2024) and comprehends architectural and archaeological assets, as point
128 features. After the field survey verification, the list of the assets included in the MIC database could be modified, possibly
129 adding, and also disregarding some assets, as explained in Sect. 2.2.2. Once the database of CH is obtained, the
130 identification of the assets potentially damaged by the flood is accomplished through the availability of the map of flooded
131 areas (shapefile format) that is freely available for download from the Copernicus Emergency Management Service
132 (COPERNICUS Emergency Management Service – Mapping, 2022). The flood map generation is based on the
133 acquisition, processing, and analysis, in rapid mode, of satellite imagery and other geospatial raster and vector data
134 sources. The identification of potentially damaged assets is obtained by overlaying the shapefiles of the flooded area and
135 the CH database in a GIS environment. In this way, it is possible to obtain a database of CH assets affected by a flood
136 event, which contains key information, such as name, type, and geo-localization of each individuated asset.

137 **2.2.2 Post-event field data collection**

138 In addition to the CH assets identified as described in Sect. 2.2.1, other assets can be considered and then added to the
139 database based on feedback from local authorities. Indeed, based on the purpose of the work, immovable and movable
140 assets characterized by aesthetic, historical, testimonial, and municipal value, as well as those with tourist or local
141 significance identified by local authorities, are considered. On the other hand, the assets listed in the MIC database that
142 are not mentioned by local authorities and by official tourism websites or have no reviews on major platforms (e.g.,
143 TripAdvisor and Google), could be excluded.

144 A novel procedure for data collection aimed at assessing the damage to CH as a result of flooding has been conceptualized.
145 The data collection forms implemented by Molinari et al. (2014) for residential buildings and industrial facilities were
146 modified and adapted to the characteristics of CH. Besides the information about the asset, the flood event (e.g., maximum
147 water level), the presence and typology of any movable artworks, and the observed physical damages, the form allows
148 for the registration of the cultural value of the CH. Table 1 summarizes the information collected on the field, through the
149 survey form.



150 **Table 1 - Survey form: description of CH assets and aspects considered.**

Form type	Description of CH	Aspects
General information		
	General features of CH	Geographic coordinates or address CH denomination Level of listing Typology of CH Current use Cultural value Property Fieldworker
	Building features	Period of construction Building structure External ornamental elements N° of floors and building height
	Description of flood characteristics	Duration Max. water level outside the building Max. water level inside the building Sediments grain size or contaminants
	Identification and type of damage	Structural, loss of accessibility Features damaged
Building internal damage		
	Damage to floors (exposure/vulnerability of the containing building)	Covered and uncovered surface Level of maintenance Presence and type of plants Damage to frescoes and wall paintings, doors and windows, floors, plants
Contents damage		
	Identification of movable assets	Presence and type of artworks
	Damage to the artworks (exposure/vulnerability of contents)	Damage to furniture, paintings, sculptures, books, decorative items, votive and liturgical elements, textile, archaeological finds

151 The form also reports the measure of “Max. water level outside the building” (see the general information form of Table
 152 1). This task refers to the on-site evaluation of the maximum height reached by water around the damaged CH assets as
 153 a result of the river overflow (hereafter MWL). The measurement for each asset can be obtained by taking as a reference
 154 a point along the perimeter where mud marks were still visible at the time of the field campaigns. In case variations in the
 155 maximum level are evident around the perimeter of the building, multiple measurement points can be noted, and then the
 156 average height value can be determined. The height of the mud marks from the ground can be measured with the use of
 157 a classical meter and/or laser distance meter. The chosen reference level (i.e., the relative level of 0 for each asset) is
 158 usually in a flat area whose coordinates will be easily found for subsequent office analysis. Indeed, referring to the
 159 measurement of the maximum height reached by the water to a reference level is necessary to correctly locate the data
 160 collected on a GIS system. Therefore, the difference in height between the maximum level reached by the water outside
 161 the considered CH asset and the reference level is measured. Practically, an operator, using a laser distance meter, points



162 horizontally from the measurement level to the reference level, while another field operator located on the reference point,
 163 can measure the height of the laser from the ground level. In the case of a bridge, the reference level from which the
 164 MWL is measured corresponds to the deck.

165 As concerns the cultural value assignment, the following procedure is adopted. Based on the qualitative descriptors
 166 introduced by Historic England (HE, 2008), non-extractive and non-use values were outlined in four categories:
 167 evidential, historical, aesthetic, and communal value:

- 168 • Aesthetic value: includes aspects of sensory and intellectual stimulation from the CH.
- 169 • Historical value: derives from the connection between the past and the present through the asset. It includes (i)
 170 illustrative value if the asset illustrates something unique or rare and (ii) associative value if it is associated with
 171 a notable family, person, or event.
- 172 • Evidential value: derives from the potential of the asset to yield evidence about past human activity.
- 173 • Communal value: derives from the meanings of a place for the people who relate to it, or for whom it figures in
 174 their collective experience or memory. It encompasses (i) commemorative value, (ii) social value, and (iii)
 175 spiritual value.

176 Each category of value can be described by four qualitative levels ranging from unknown to high value: the respective
 177 “V” score was assigned to each asset. It is noteworthy that the chosen hierarchical system excludes the “no value” level,
 178 preferring to assign an “unknown value” to the asset without evidence that would support its significance. Table 2
 179 summarizes, for each category of value, the criteria to be considered when assessing the level of value of the cultural
 180 property and the scores corresponding to each class of value.

181 **Table 2 - Classification and criteria to define intangible value of CH with their respective class and associated score.**

Type of value	Criteria to assign CH value	Class value and score (V)
Aesthetic	Valuable structure (e.g., architectural art using local materials or high-value import materials); valuable artworks inside (objects of outstanding workmanship, precious votive elements)	High (10)
	Valuable structure or valuable artworks	Moderate (7)
	No uncommonly attractive qualities, but that display particular characteristics of an identified style	Limited (3)
	No valuable characteristics or stylistic features	Unknown (0)
Historical	Proved illustrative and associative value or pre-1800 structure	High (10)
	1800 structure	Moderate (7)
	1900 structure	Limited (3)
	Structures under 70 years of age	Unknown (0)
Evidential	Physical remains of past human activities. The current use has not deleted proofs of the past	High (10)
	No evidence of the past, but their history is based on past human activity	Moderate (7)
	Only the denomination recalls past human activity	Limited (3)



	No linked to past human activities	Unknown (0)
	Spiritual, social, or commemorative value. Additionally, committees have been founded to promote or defend the asset, or the asset is linked to a specific local tradition	High (10)
Communal	Spiritual, social, or commemorative value. No committees or traditional events are linked to the asset	Moderate (7)
	Limited spiritual value (e.g., place of worship with sporadic openings). No traditional events are linked to the CH	Limited (3)
	No spiritual, social or commemorative value	Unknown (0)

182 Following Romao and Paupério (2021), the baseline pre-disaster intangible value BV of a certain CH asset will then
 183 correspond to the sum of the scores established for each type of value given by:

$$BV = \sum_{i=1}^4 V_i \quad \text{Eq. 1}$$

184 where V_i is the score of i th typologies of value.

185 2.2.3 Ex-post damage assessment

186 The level of damage is obtained by combining loss in tangible and in intangible values. Loss in tangible value is strictly
 187 linked to the observed physical damages and to the costs of restoration. It includes structural and non-structural damage.

188 The Italian Civil Protection Department defines structural damage as those involving the load-bearing elements of the
 189 building, such as pillars, beams, and slabs. In case of non-structural damage, the elements that do not affect the stability
 190 of the building such as ceiling and floor finishes, plumbing, and electrical systems are affected.

191 On the other hand, loss in intangible value is established by evaluating flood indirect impacts. Loss in aesthetic value
 192 refers to the effectiveness of restoration in allowing the community to be sensorial stimulated by the asset again. The
 193 impact on historical and evidential values depends on how the flood impacted the original structure and materials or the
 194 proofs of past human activities, such as plaques or archives. Finally, the loss in communal value is measurable as the
 195 duration of inaccessibility of the asset (HE, 2008). In this paper, we assume that an asset sustaining moderate damage
 196 may be closed for days or weeks for clean-up and safety check operations, whereas an asset with severe damage may be
 197 closed for months for restoration works. It is also assumed that if an asset remains inaccessible for more than one year
 198 the loss in intangible value is comparable to the destruction, as the community will move to a new place to express
 199 communal value.

200 Damage is categorized into four hierarchical classes, with each asset assigned both a loss in tangible value (LTV) and a
 201 loss in intangible value (LIV). LTV ranges from 5 to 30, while calculating LIV involves applying the methodology
 202 outlined in Romao and Paupério (2021). This method employs a coefficient (D), which spans from 0 to 1, associated with
 203 each class of loss or damage. Then, for each cultural heritage asset, the loss in LIV is defined applying Eq. 2:

$$LIV = \sum_{i=1}^4 V_i \times D_i \quad \text{Eq. 2}$$

204 where V_i represents the score of the category of values. As shown in Table 2, the score of V ranges from 0 to 10, while
 205 the coefficient D (Table 3) could be at most equal to 1, resulting in a LIV score that ranges from 0 to 40. This implies,



206 therefore, that greater weight is given to *LIV* than to *LTV* to emphasize the peculiar contribution of intangible aspects to
 207 the loss evaluation. The classes of damage and the criteria adopted to define losses value, considering both tangible and
 208 intangible features, are reported in Table 3.

209 **Table 3 - Classes of damage and definition of *LTV* and *LIV*.**

Classes of damage	<i>LTV</i>	<i>LIV</i>
Undamaged or slightly damaged	CH can return to its original state with deep cleaning. <i>LTV</i> =5	The intangible values have not been impacted. The site has never been closed off. <i>D</i> = 0
Moderately damaged	Slight structural and non-structural damages (door unhinged, appliances damaged, and presence of mold). <i>LTV</i> =10	Restoration can repair most of the features that provide aesthetic, historic, or evidential value. The site has been closed for days or weeks. <i>D</i> = 0.3
Severely damaged	Building and artworks damaged (wrecked floor, wall painting, sculptures, paintings, furniture, wooden choir, pipe organ, liturgical supply ruined). <i>LTV</i> =15	Despite restoration works, the damaged features that hold aesthetic, historical, and evidential significance cannot be fully restored to their original state. The site has been closed for months. <i>D</i> = 0.7
Destroyed/lost	Asset destroyed (the building materials are not on site anymore). <i>LTV</i> =30	Lost in significance. The site or its most relevant features are destroyed and/or closed for more than one year. <i>D</i> = 1

210 **2.2.4 Factors influencing flood damage**

211 Flood damage to buildings can be caused by several factors, both intrinsic, influenced by the properties of the structure
 212 itself, and extrinsic, influenced by the dynamics of the flood event. In literature, the following factors are typically
 213 considered: intrinsic factors, such as the material of construction, the presence of contents susceptible to flood damage
 214 and with significant cultural value, the existence of possible water communication between the building and the river, the
 215 presence of defence elements, age in years of the building, number of floors, building shape, building orientation in
 216 respect to the water flow, state of conservation of the building, and objects that drag the sheet of water; extrinsic factors
 217 such as maximum water level outside the building, flow velocity, hydrodynamic pressure, flood duration, presence of
 218 sediments, and contaminations (e.g., Smith, 1994; Kreibich and Thieken 2008; Dall’Osso et al., 2009; Dutta et al., 2011;
 219 Galasso et al., 2021; Marin Garcia et al., 2023).

220 These factors can be directly assessed by means of post-event field survey, or by the interpretation of post-event photos
 221 and videos and can be classified based on the level of difficulty in obtaining them (Marin Garcia et al., 2023).

222 Additionally, other authors (e.g., Cuca and Barazzetti, 2018; Di Salvo et al., 2018; Kefi et al., 2020; Al-Kindi and Alabri,
 223 2024) also consider some geospatial factors as they could influence buildings damage: difference between the level of the
 224 ground floor of the building and the riverbank, distance between river and building, difference between DTM and filled
 225 DTM, local slope, curvature, topographic wetness index (Beven and Kirkby, 1979), stream power index (Moore et al.,
 226 1991), terrain ruggedness index (Riley et al., 1999), and NDVI.



227 The relationship between MWL and structural damage is well-known in the literature. For its evaluation, post-event field
228 survey measurements are necessary (as described in Sect. 2.2.2). On the other hand, the evaluation of the geospatial
229 factors requires the use of source data in vector (e.g., hydrographic network, and buildings) and raster formats (e.g.,
230 DEM), which are generally available from national or regional databases. Concerning the DEM spatial resolution, the
231 degree of damage to buildings could result from small variations of the morphology. For this reason, the use of high-
232 resolution DEM (cell size ranging between 1×1 m and 5×5 m) is recommended, especially in the case of urban flood
233 analysis (Mark et al., 2004; Adeyemo et al., 2008; Di Salvo et al., 2018).

234 Specific procedures using GIS tools are implemented to assess two factors: the minimum distance (ΔD) between a CH
235 asset and the river, and the elevation difference (ΔE) between the CH asset and the riverbed. First, polygon-type shapefile
236 of the buildings corresponding to CH assets are identified. For ΔD , the centroid of the building polygons is considered,
237 with the river network as the reference for distance evaluation. Using the centroid of the buildings and the nearest point
238 on the hydrographic network, the ΔD factor is determined automatically with GIS tools (e.g., the Near tool in Analysis
239 Tools of ESRI™ ArcGIS Pro™). Concerning ΔE , for each building polygon, the DTM is extracted. The elevation
240 difference between the CH asset and the nearest point feature on the riverbed is then calculated. To refine the riverbed
241 elevation, a buffer distance around the riverbed can be considered.

242 Concerning the river slope factor (RS), we assume that the average slope of the riverbed is a reasonable proxy for the
243 river flow velocity, which is difficult to estimate in the absence of instrumented sections or video recordings during a
244 flood. Moreover, the slope of the river also influences the transport of sediment and the grain size, which in turn can affect
245 the degree of damage. Based on our best knowledge, there are no specific recommendations for RS evaluation in the
246 literature. In this paper, the average slope of 500 m and 1000 m upstream stretch with respect to the assets, is considered.
247 Regarding the other geospatial factors, these can be evaluated as indicated by the relevant literature cited above. To
248 evaluate the relationship between each contributing factor and the tangible and intangible losses, the mean and median
249 values of the area of each CH asset polygon are considered.

250 3 Case study

251 The method is applied to CH assets damaged by the 15-16 September 2022 flood in the Marche Region. This section
252 includes an overview of the basins, along with a general description of the municipalities and their historical significance
253 (Sect. 3.1). Moreover, the dynamics of the intense rainfall event and associated flooding are described in Sect. 3.2.

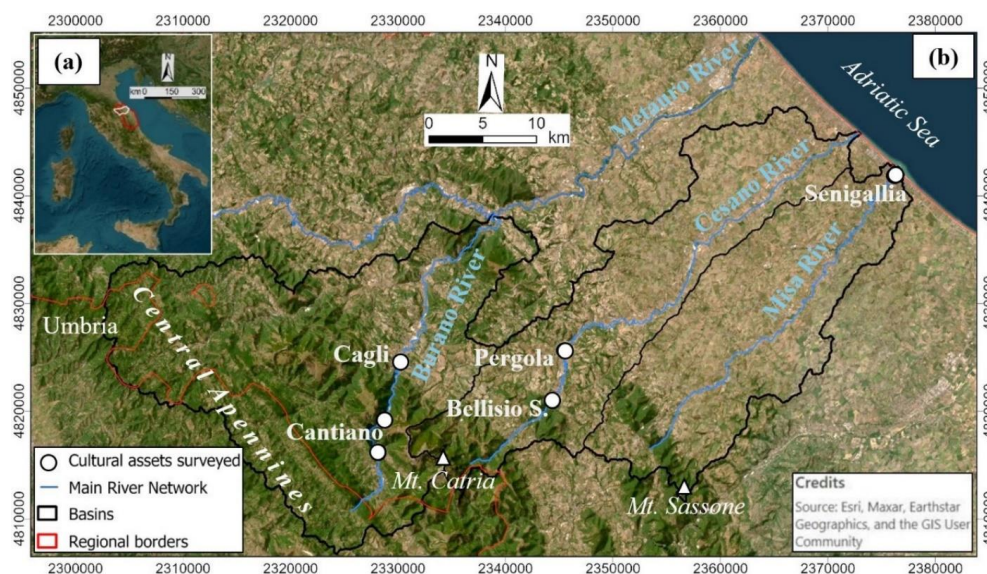
254 The geospatial data utilized for the analyses outlined in Sect. 2.2 were sourced from official regional and national
255 databases. Vector data and the numerical technical map of the Marche Region (“CTR”, scale 1:10000) were obtained
256 freely from the Marche regional cartographic data portal (REGIONE MARCHE, Ambiente, 2023). The LiDAR-derived
257 DEM, with a spatial resolution of 1 m and vertical accuracy of 0.15 m (comprising both DSM and DTM data), was
258 acquired following a request to the Italian Government's "Ministero dell'Ambiente e della Sicurezza Energetica" (MASE,
259 Geoportale Nazionale, 2024). Specifically for the coastal area of Senigallia, a portion of the LiDAR data utilized had a
260 spatial resolution of 2x2 meters.

261 3.1 Overview of the study areas

262 The CH assets damaged by the flood are distributed across three basins on the eastern slope of the Central Apennine chain
263 of the Marche Region, in Central Italy (Figure 1a,b). The basins are drained by their respective main rivers, namely
264 Burano (a right tributary of the Metauro River), Cesano, and Misa (Figure 1b). The highest peak of the study area, Mt.



265 Catria (1704 m a.s.l.), is situated at the watershed between the Burano and Cesano basins. The highest peak of the Misa
266 basin corresponds to Mt. Sassone, reaching an elevation of 826 m a.s.l. (Figure 1b).
267 The CH assets damaged by the flood are included in the municipalities of Cantiano and Cagli (Burano basin), Pergola
268 and the hamlet of Bellisio Solfare (Cesano basin), and Senigallia (Misa basin), in Pesaro-Urbino and Ancona provinces.
269 These localities exhibit diverse historical and cultural attributes. The historical significance of Cantiano and Cagli is
270 notably linked to the ancient Roman road known as the "Flaminia," which was inaugurated between 223 and 202 B.C.
271 (Clini et al., 2023). One noteworthy site from the Roman period along the Via Flaminia is the Ponte Grosso bridge,
272 represented by the white dot between Cantiano and Cagli (Figure 1b).



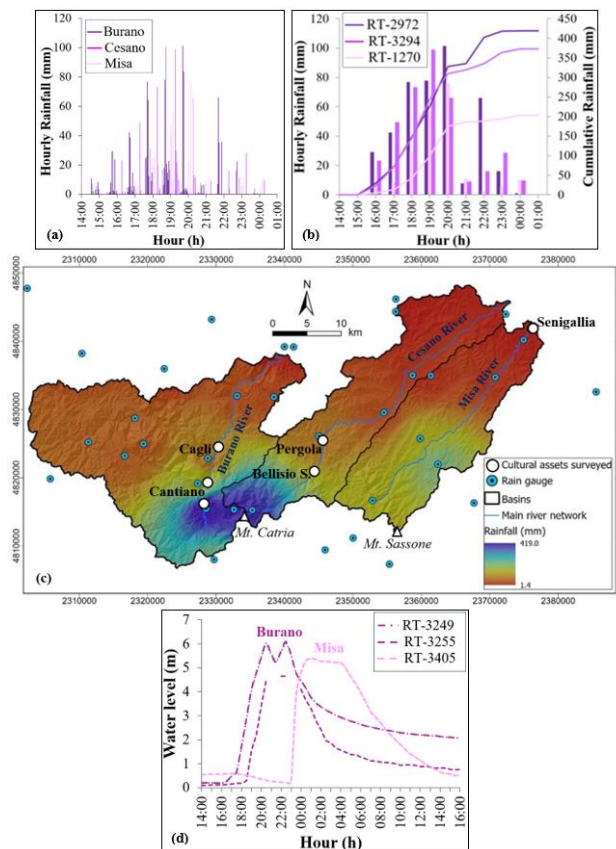
273
274 **Figure 1.** (a) The study area in Central Italy. In red is the border of the Marche Region, and in white is the area of the basins which
275 includes the assets involved during the flood that occurred on 15-16 September 2022. (b) The three basins that include the assets
276 affected by the flood: Burano, Cesano, and Misa. Coordinate system: WGS 1984 UTM Zone 33N.

277 As for the Cesano basin, the site of Bellisio Solfare has a recent history starting from the late 1800s, with the beginning
278 of construction of the sulfur refinery. This location holds significance as part of the Marche Mining Geopark, established
279 in 2001 (Sulphur, MARCHE MINING GEOPARK, 2024). Pergola, known as the “city of hundred churches”, has been
280 inhabited since Prehistory, with the cultural heritage most extensively documented originating from the Roman period.
281 The city of Senigallia has a rich historical background, as it was the first Roman colony to settle in the Adriatic coastal
282 plain. In the realm of flood risk management, the origins of protective measures can be traced back to the early Roman
283 settlements (De Donatis et al., 2019). Notably, the interventions were directed toward the construction of walls along the
284 course of the Misa River, with the dual function of both military and flood defense of the Senigallia city. The construction
285 of the walls, as well as other changes to the minor hydrographic network carried out by the Romans, preserved the city
286 from flooding by the Misa River. However, during the post-Roman age, the dismantling of these walls exposed a
287 significant portion of the city to floods, as evidenced by the event in 1472 and subsequent flooding between the 16th and
288 18th centuries A.D. The aftermath of these post-Roman age flood events, combined with continuous human interventions
289 contributed to shaping the current topography of the urban area in Senigallia (De Donatis et al., 2012).



290 **3.2 The 15-16 September 2022 flood event**

291 On 15-16 September 2022, following an extended period of drought in the preceding months (Pulvirenti et al., 2023), the
292 Northern Marche Region experienced very intense rainfall due to the formation of a stationary self-regenerating
293 thunderstorm system over the Apennine mountains, resulting in disastrous floods. From early afternoon on 15 September,
294 rainfall started to affect the Mt. Catria area, until it also extended to the mountainous areas of the Burano, Cesano, and
295 Misa basins. In Figure 2 the rainfall and hydrometric data of the event are reported. The data were downloaded from the
296 Civil Protection monitoring system website of the Marche region (SIRMIP ON-LINE, 2024) and then elaborated.



297 **Figure 2.** Observed rainfall and flow rate of the 15-16 September 2022 event. a) Hourly rainfall measured by the rain gauges in the 3
298 basins; b) The 3 rain gauges* of each basin that measured the maximum cumulative rainfall; c) Map of the cumulative rainfall; d)
299 Measured water level by hydrometer** of the Burano River and Misa River. *Rain gauges codes: “Cantiano RT-2972” (Burano basin);
300 “Monte Acuto RT-3294 (Cesano basin)”; “Colle RT-1270” (Misa basin). **Hydrometers codes: “Pontedazzo RT-3249” (1 km
301 downstream Cantiano, Burano River) and “Cagli Ponte Cavour RT-3255” (Burano River); “Ponte Garibaldi RT-3405” (Senigallia,
302 Misa River). The shaded relief basemap of panel (c) was obtained from the TINITALY DEM (Tarquini et al., 2007, 2023). Distributed
303 under the CC BY 4.0 license. Coordinate system: WGS 1984 UTM Zone 33N.
304

305 The most intense phase of the event occurred between 18:00 and 19:00, with maximum hourly peaks of about 100 mm
306 recorded by stations near Mt. Catria, at the watershed between Burano and Cesano basins. In the Misa basin, the maximum
307 hourly peak was recorded at 19:30, amounting to about 80 mm (Figure 2a,b).



308 The map of Figure 2c, obtained interpolating the rain gauges data using the inverse distance weight interpolation method
309 (Shepard, 1968) in ESRI™ ArcGIS Pro™ (IDW tool in Spatial Analyst Tools), highlights the high spatial variability of
310 the rainfall event.
311 The rain gauges surrounding Mt. Catria, at the watershed between the Burano and Cesano basins, recorded the highest
312 hourly rainfall intensity and cumulative rainfall, reaching 420 mm in 12 hours. In contrast, in the Misa basin, the maximum
313 cumulative rainfall recorded northeast of Mt. Sassone is half the amount that has rained in the Mt. Catria area. In just 6
314 hours, about half the precipitation that typically occurs on average in a year (i.e., 780 mm, REGIONE MARCHE,
315 ANNALI IDROLOGICI, 2021) fell in the mountainous areas of the Burano, Cesano, and Misa basins. A return period of
316 > 1000 years has been estimated for rainfall durations of 3-6-12-24 hours at the rain gauges located in areas characterized
317 by higher rainfall intensities (REGIONE MARCHE, RAPPORTO DI EVENTO preliminare, 2022).
318 Although about half as much rain fell in the Misa basin as in the Burano and Cesano basins, the effects were still
319 disastrous. One reason can be attributed to the different geology of the basins (e.g., Iacobucci et al., 2022). The Mt. Catria
320 ridge in the Burano and Cesano basins mainly consists of fractured carbonate rocks, that contribute to the infiltration
321 processes (Mastrorillo and Petitta, 2014), mitigating flood effects. On the other hand, the Misa basin is mainly composed
322 of clays and sandstones, which are less permeable. As a result, a larger portion of the rainfall contributed to runoff
323 processes, exacerbating flood dynamics.
324 The hydrometers reported in Figure 2d, in the Burano basin, are located in the Pontedazzo section which is 1 km
325 downstream from Cantiano (RT-3249), and in Cagli (RT-3255). The intense rainfall that fell over a brief period led to an
326 abrupt increase in the river discharge, as highlighted by the water level variations of the Burano and Misa rivers (Figure
327 2d). The blockage of bridges and culverted stretches significantly contributed to the flooding. In Cantiano, the flooding
328 of the urban centre occurred from the culverted section of the Burano River, as shown in some videos recorded by
329 residents (e.g., *World Events News*, 2022). In the case of Senigallia, a video shows the evolution of the flooding of the
330 Misa River (*Storm Chasers Marche*, 2022). In this case, large woody debris crashed against the deck of the bridges "Corso
331 2 Giugno" and "Garibaldi" (where the hydrometer is located), causing widespread flooding throughout the city.
332 A total of 13 people died, and severe damage resulted in most settlements along the main rivers. Further details on flood
333 dynamics in Cantiano, Cagli, Pergola, and Senigallia, and the consequent damage to CH assets, are provided in Sect. 4.2
334 of the results.

335 4. Results and discussion

336 The results of applying the proposed method to assess the damage to CH assets caused by the flood event that occurred
337 on 15-16 September 2022, in the Burano, Cesano, and Misa basins, are presented and discussed in two main sections.
338 Sect. 4.1 concerns the analysis of the results obtained by applying the ex-post damage assessment method, which is the
339 main goal of this paper. In Sect. 4.2 the results of the ex-ante application are compared with the ex-post results and then
340 discussed.

341 4.1 Ex-post damage assessment

342 4.1.1 Features of the CH assets and losses assessment

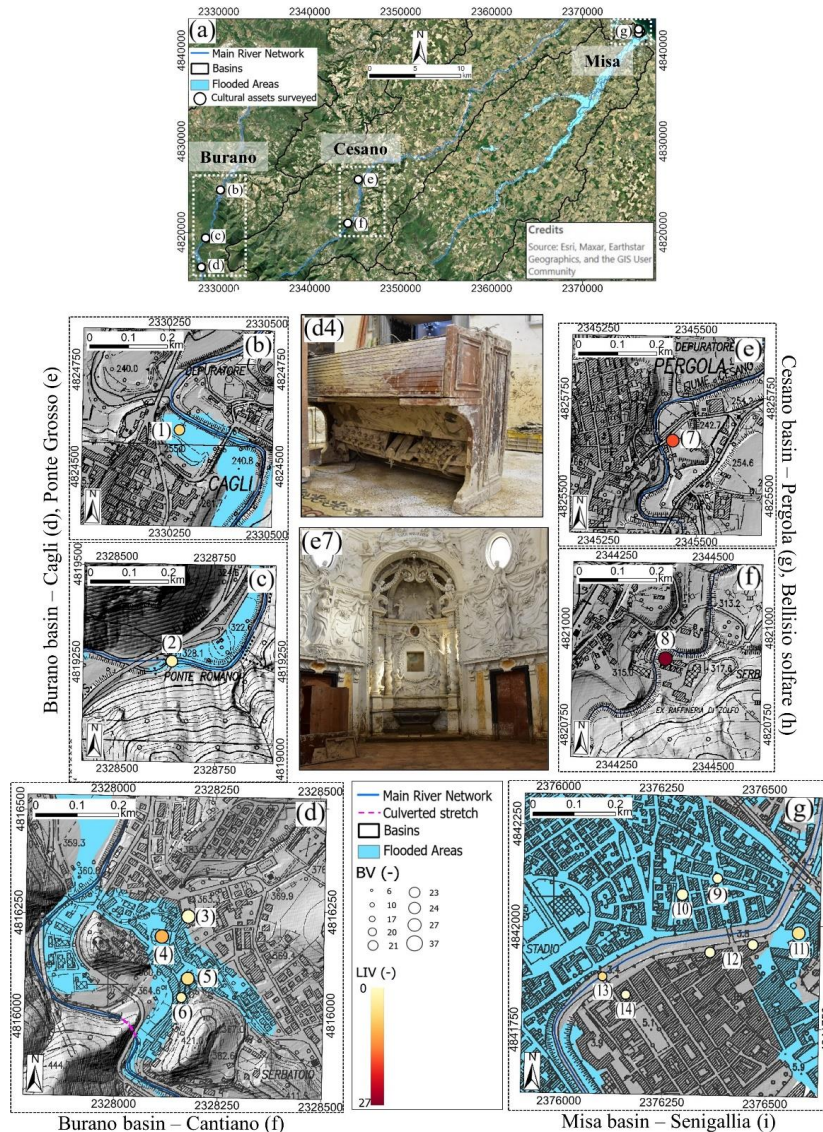


343 Through remote analysis and field survey verification, the list of CH assets actually damaged by the flood was obtained.
 344 A total of 14 assets were identified, for which, maximum water level (MWL) baseline value (*BV*), and both losses in
 345 intangible (*LIV*) and tangible (*LTV*) scores are provided in Table 4. Most of the damaged CH assets are religious building
 346 types (6 out of 14), while the remaining damaged assets include bridges, a fortified gate, a square, a porch, and residential
 347 or industrial architecture.

348 **Table 4 – CH assets damaged by the flood, classified by basin, type, MWL, and the associated scores of *BV*, *LIV*, and *LTV*.**
 349 **Can: Cantiano; Cag: Cagli; P: Pergola; BS: Bellisio Solfare. All the assets in the Misa basin are located in Senigallia.**

Basins	CH assets	Type	MWL (m)	<i>BV</i> (-)	<i>LIV</i> (-)	<i>LTV</i> (-)
Burano	(1) S. Emidio oratory (Cag)	Church	2.40	20	7	10
	(2) Ponte Grosso (Can)	Bridge	2.50	23	2.1	10
	(3) S. Agostino church (Can)	Church	0.35	27	0	5
	(4) S. Giovanni Battista collegiate (Can)	Church	1.40	27	13	15
	(5) S. Nicolò church (Can)	Church	2.05	24	5.1	10
	(6) Historical buildings Via Fiorucci (Can)	House	2.30	17	2.1	10
Cesano	(7) S. Maria delle Tinte church (P)	Church	3.40	37	20	15
	(8) Bellisio Solfare refinery (BS)	Factory	2.66	27	27	30
Misa	(9) Porta Lambertina	Fortified gate	0.44	17	0	5
	(10) S. Maria del Porto church	Church	0.70	21	0	5
	(11) Foro Annonario	Square	0.65	24	4.5	5
	(12) Portici Ercolani	Porch	1.50	17	0	5
	(13) Ponte Garibaldi	Bridge	2.18	6	6	15
	(14) Filanda Serica	Factory	0.23	10	0	5

350 Figure 3a shows the general view of the basins, and panels b-g highlight the distribution of the *BV* and *LIV* scores for the
 351 sites of the three basins, while Figure 4 reports the distribution of the *LTV* scores throughout the basins (panels b-g);
 352 panels b1-g2 depicts two examples how the MWL was estimated during the field survey, in the case of a generic building
 353 and a bridge, respectively; and in panels b1-c2 are reported two post-event photos showing the MWL.
 354 The most valuable cultural asset corresponds to the S. Maria delle Tinte Church ($BV = 37$), which is located in Pergola,
 355 within the Cesano basin (Figure 3, panel e7). The maximum aesthetic, historical, and communal values are assigned to
 356 that asset, as the church was adorned with statues and stucco decorations, in addition to precious 18th-century wooden
 357 pews, painted with floral motifs. Moreover, the church was built at the behest of the historical dyers and wool merchant
 358 guild, and still today it is a representative place in the city. Indeed, after the 2022 flood, a committee called “Gli Angeli
 359 delle Tinte” was assembled to propose a restoration project for the church (GLI ANGELI DELLE TINTE, 2024). In
 360 general, religious architectures were built before the 1800s and, in addition to the high spiritual value, valuable structures
 361 and valuable artworks coexist, resulting in a high aesthetic value. For these reasons, the average intangible value score of
 362 the damaged churches is relatively high ($BV = 26$), in confront with the average score of the other asset types ($BV =$
 363 18).
 364 Ponte Garibaldi (Figure 3a panel g13), namely the damaged bridge in Senigallia (Misa basin), has the lowest intangible
 365 value ($BV = 6$) for its limited historical value (it dates to the 20th century), as well as for its limited aesthetic value.
 366 Indeed, even if it is an example of the typical early 20th-century architectural style, it is not a valuable structure. On the
 367 other hand, the other damaged bridge in the Burano basin, Ponte Grosso in Cantiano (Figure 3a, panel 3c), is characterized
 368 by a higher intangible value ($BV = 23$). In this case, even if its aesthetic value is limited, both the historical and evidential
 369 values are high, because it is a rare example of infrastructure of the Ancient Rome Empire.



370

371 **Figure 3.** (a) General view of the CH assets surveyed for each basin; (b-g) the maps showing the BV (graduate symbols) and LIV (scale
 372 colors) scores of the assets. Burano basin: (b) S. Emidio oratory in Cagli (1), (c) Ponte Grosso in Cantiano (2), and (d) the assets in
 373 Cantiano (3-6); Cesano basin: (e) S. Maria delle Tinte Church (7), and (f) Bellisio Solfare (8); Misa basin: (g) the assets in Senigallia
 374 (9-14). Panels d4 and e7 report post-event photos of S. Giovanni Battista collegiate and S. Maria delle Tinte church where damage as
 375 a result of mud deposition inside the buildings is visible. The shaded relief basemap of panels (b-g) was obtained from the DTM LIDAR
 376 of the Ministero dell'Ambiente e della Sicurezza Energetica (MASE, Geoportale Nazionale, 2024). The numerical technical map of
 377 panels (b-g) is from the Marche Region (REGIONE MARCHE, Ambiente, 2023). Both maps are distributed under the CC BY 4.0
 378 license. Coordinate system: WGS 1984 UTM Zone 33N.

379

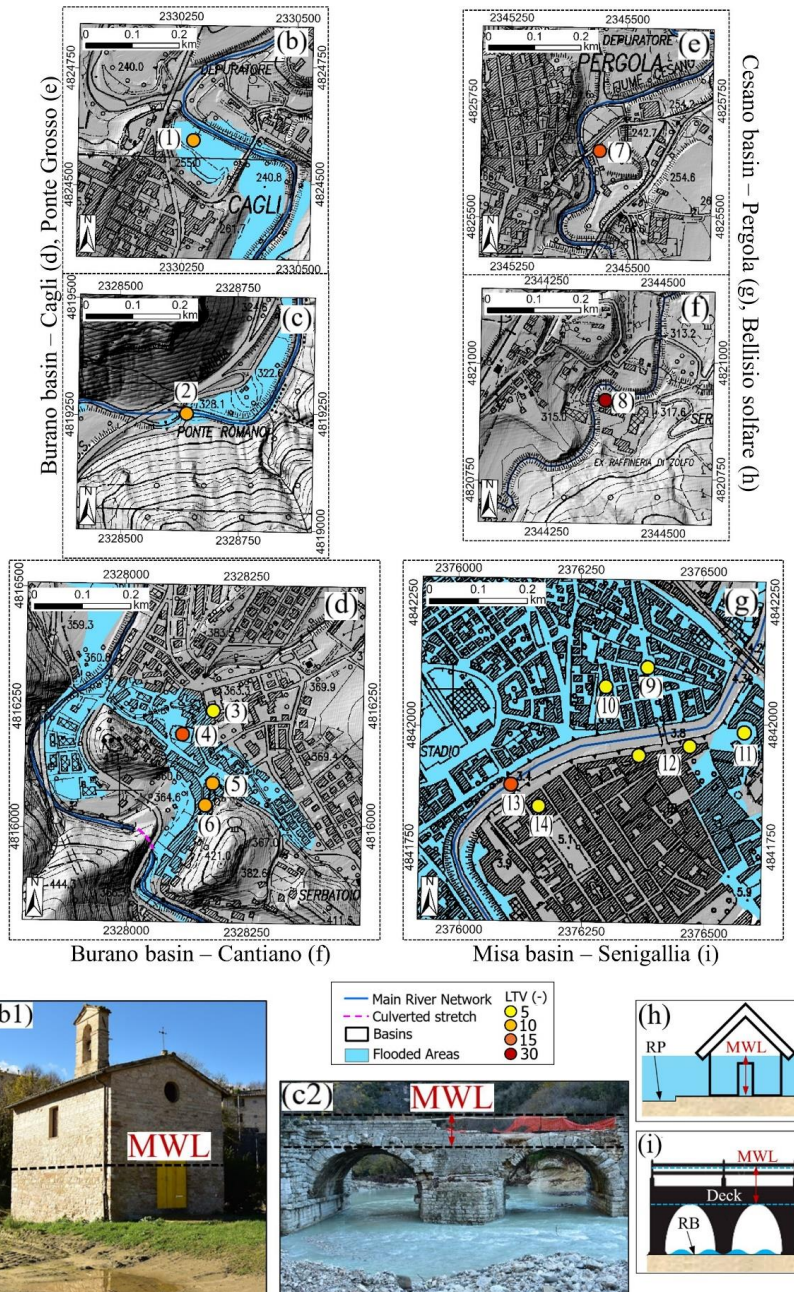
380 It is worth noting that the Bellisio Solfare refinery asset (Figure 3a, panel f8), despite being mostly unknown among the
 381 most important tourist attractions and with a poor state of conservation, is characterized by high intangible value (BV =
 382 27). Indeed, it represented an important proof of the past industrial activity of the Pergola municipality area (Burano
 383 basin). Furthermore, a high communal value is assigned to it, due to the presence of an organization that aims to rebuild
 the asset.



384 The assets of Historical Buildings Via Fiorucci (Figure 3a, panels d5) and Porta Lambertina (Figure 3a, panel g9) are
385 distinguished by their high historical significance, being notable architectures of the past, and holding a moderate aesthetic
386 appeal, resulting in a $BV = 17$. In contrast, Foro Annonario (Figure 3a, panel g11) and Portici Ercolani (Figure 3a, panel
387 g12), are CH open spaces of notable value, with $BV = 24$, and 17, respectively. While these two assets share similar
388 evaluations across most value types, the Foro Annonario holds significant community value. Indeed, it represents the
389 historical central marketplace of Senigallia, thus remaining a vital meeting point for the city since its realization.

390 Moreover, Figure 3a (panels b-g) reports the extension of the flooded area from the Copernicus agency. In general, these
391 maps agree with those actually flooded as a result of the event (the same for Figure 4). The only exceptions are the areas
392 of Pergola and Bellisio Solfare, as well as assets #12,14 in Senigallia. This demonstrates that these maps are useful for
393 rapid identification of flooded areas. However, a direct field evaluation to establish which assets were effectively flooded
394 is fundamental.

395 In Figure 4 are reported the maps showing the spatial distribution of the LTV scores of each asset (panels b-g). Concerning
396 the Bellisio Solfare refinery (Figure 4, panel f8), the highest LIV and LTV were assigned as the flood destroyed completely
397 the building, and during the survey, only ruins were observed ($LIV = 27$, and $LTV=30$). The historic S. Maria delle Tinte
398 church (Figure 4, panel e7) sustained considerable damage caused by the flood, both in terms of damage to intangible and
399 tangible value ($LIV = 20$, and $LTV=15$). The inundation resulted in harm to the electricity system and the emergence of
400 mold on both the floor and wall paintings. Additionally, the force of the floodwater partially wrecked the door and
401 destroyed the 18th-century pews. As a result, the aesthetic value of the church was deemed lost. Moreover, its extended
402 closure period led to a significant impact on its communal value. Even the S. Giovanni Battista collegiate (Figure 4, panel
403 3f) experienced severe damage ($LIV = 13$, and $LTV=15$). In addition to the effects already observed for the other assets,
404 floor tiles were broken, the wooden choir and altars were swollen due to the floodwater, and the 16th-century liturgical
405 supply was covered by mud. In the case of S. Nicolò church (Figure 4, panel d5), part of the floor collapsed, and the
406 external stone and metal balustrade were swept away by the flowing water ($LIV = 5.1$, and $LTV=10$). Similar loss scores
407 were observed for the St. Emidio oratory (Figure 4, panel b1), in which, however, a significant loss was due to the wooden
408 door as it was swept away.



409

410 **Figure 4.** (d-i) The maps of the LTV scores of the assets. Panels (b1) and (c2) display the post-event field survey photos depicting the
 411 damage to the S. Emidio oratory and Ponte Grosso, respectively. Panels (h) and (i) report the schematic view of the MWL estimation
 412 in the case of a generic building and a bridge, respectively (RP is the reference point used for the measurement of the MWL, and RB
 413 is the riverbed). The shaded relief basemap of panels (b-g) was obtained from the DTM LIDAR of the Ministero dell'Ambiente e della
 414 Sicurezza Energetica (MASE, Geoportale Nazionale, 2024). The numerical technical map of panels (b-g) is from the Marche Region
 415 (REGIONE MARCHE, Ambiente, 2023). Both maps are distributed under the CC BY 4.0 license. Coordinate system: WGS 1984
 416 UTM Zone 33N.



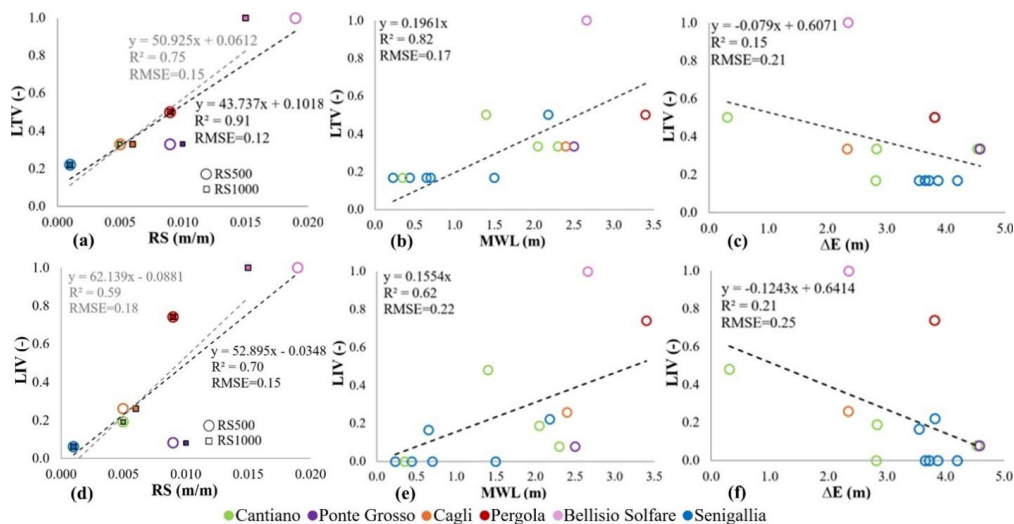
417 Overall, a high level of losses was observed for most of the affected religious structures, where closure due to extensive
418 damage contributed to a decrease in communal value. Conversely, the S. Agostino (Figure 4, panel d3), and Porta
419 Lambertina, S. Maria del Porto, Portici Ercolani, and Filanda Serica assets (Figure 4, panels g9,10,12, and 14) incurred
420 the lowest losses, both in intangible and tangible aspects $LIV = 0$, and $LTV=5$. Specifically, the two churches were not
421 damaged as they are over-elevated from the ground floor. For all these assets, only mud marks dirtied the external walls.
422 As regards the Foro Annonario (Figure 4, panel g11), the only damage is related to the mud marks along the porch
423 perimeter. Nevertheless, the relative LIV is higher than 0 ($LIV = 4.5$) since the circular square in which the porches are
424 located remained impracticable for some days.
425 The two affected bridges were significantly damaged as the maximum level reached by the water during the flood
426 exceeded the height of the deck. Portions of the arch stones of the Ponte Grosso (Figure 4, panel c2) collapsed leading to
427 a moderate decrease in tangible value ($LTV=10$). However, the historical and evidential aspects remained unscathed,
428 resulting in a relatively low decline in intangible value ($LIV = 2.1$). Conversely, the Ponte Garibaldi (Figure 4, panel
429 g13) sustained severe structural damage ($LTV=15$). Indeed, some months after the field survey, it ultimately had to be
430 demolished (ANSA, Regione Marche, 2023), resulting in the loss of both its aesthetic and historical significance ($LIV =$
431 6).
432 Regarding the MWL estimate (Figure 4, panels h,i), it was directly measured during the field survey, as detailed in Sect.
433 2.2.2. However, there were exceptions with the two bridges and the Bellisio Solfare refinery. Direct measurements were
434 not possible in these instances due to the inaccessibility of the bridges, compounded by the destruction of the Bellisio
435 Solfare asset. Consequently, for these cases, the estimation of MWL was conducted indirectly.
436 As for the Ponte Grosso (Figure 4, panel c2), the MWL was estimated considering wood deposition height at road signals
437 close to the bridge (e.g., video from TGC0M24, 2022). The resulting estimated MWL from the deck is 2.5 m.
438 With regards to Ponte Garibaldi (Figure 4, panel g13), the highest water level value from the riverbed was recorded during
439 the flood peak by the hydrometer on the Misa River (i.e., 5.39 m as reported in Figure 2d). The height from the riverbed
440 to the base of the deck was estimated, and this value was subtracted from the maximum height measured by the
441 hydrometer, resulting in a MWL of 2.18 meters.
442 In the case of the Bellisio Solfare asset (Figure 4, panel f8), the MWL was estimated by considering the mud marks height
443 at the closest building on the hydrographic left of the Cesano River. The measured MWL at this building, used as a
444 reference, is 1.45 m. Thus, considering the DTM difference between the refinery and this site, the resulting MWL at
445 Bellisio Solfare is equal to 2.66 m.

446 4.1.2 Factors influencing flood damage

447 In this study, the following factors were considered as those that can potentially contribute to the damage to CH assets:
448 maximum water level outside the building (MWL), minimum distance between asset and river (ΔD), difference between
449 the elevation of CH asset and the elevation of the riverbed (ΔE); difference between DTM and filled DTM (ΔDTM),
450 average slope of the river (RS), local slope (LS), curvature (CU), Topographic Wetness Index (TWI), Terrain Ruggedness
451 Index (TRI).
452 The procedures described in Sect. 2.2.2 allowed us to investigate which factors contributed significantly to both the LTV
453 and LIV of the CH assets. Among all the factors analyzed, RS, MWL, and ΔE showed some correlation to LTV (Figure
454 5a-c), while for all others the correlation proved to be negligible. The same trend resulted also correlating the LIV with
455 the same contributing factors (Figure 5d-e). This can be explained as the LIV is linked to the LTV. Indeed, if an asset is



456 destroyed, all the intangible values are lost too. Overall, there is a greater correlation between LTV and contributing
 457 factors than *LIV*, as the aspects that are not strictly related to physical parameters are considered when assessing *LIV*.
 458 The factors RS and LTV (Figure 5a), considering the 500 m stretch upstream of the single asset of a group of assets
 459 (RS500), exhibit both a higher correlation and a lower dispersion ($R^2=0.91$, RMSE= 0.12). Also considering the 1000 m
 460 stretch upstream from the CH (RS1000), the LTV-RS relationship is clear, although it results in a lower correlation and
 461 greater dispersion ($R^2=0.75$, RMSE=0.15) than considering the RS500 factor. These results show that an increase in RS
 462 corresponds to an increase in LTV. Both 500 m and 1000 m were considered as there are no clear recommendations in
 463 the literature on whether the flow of a river adapts to the slope of the riverbed. Nevertheless, considering these distances,
 464 it is reasonable to assume that the slope of the riverbed affects the energy of the flowing water and thus can be used as a
 465 valid proxy for current velocity. As observed, the dynamics of the flood event were different throughout the basins (Sect.
 466 3.2). In the case of the Misa River in Senigallia (RS500,1000=0.001 m/m), the flooding that occurred was mainly caused
 467 by the overtopping of the 2 bridges present, which in turn caused a progressive and slow rise in water levels throughout
 468 the city. This scenario resulted in damage to CH primarily attributable to water stagnation and the accumulation of fine
 469 sediments (ranging from clays to sands), rather than the direct impact of hydrodynamic forces from flowing water. Indeed,
 470 for all the CH assets, the minimum LTV (5) was observed (Table 4). The only exception is the Garibaldi Bridge, which
 471 was more severely damaged (LTV=15) as it was obstructed due to the passage of woody debris and the related pressure
 472 exerted on it. On the other hand, for the sites in the Burano and Cesano basins, a steeper slope caused greater damage due
 473 to the hydrodynamic force of the water impacting the CH assets. This is evidenced by some videos recorded at Cantiano
 474 (as described in Sect. 3.2), but especially by the destruction of the Bellisio Solfare refinery (LTV=30). In this case, the
 475 slope of the Cesano River was sufficient to transport and deposit large amounts of floating and coarse debris, including
 476 wood, gravel, and boulders, which contributed to the destruction of the site. However, it is also worth noting that this site
 477 was in a poor state of conservation, that possibly reduced structural resistance.



478
 479 **Figure 5.** Relations between normalized LTV (a-c) and *LIV* (d-e) with influencing contributing factors: (a,d) RS, considering distances
 480 of 500 m (black line) and 1000 m (grey line) upstream from the single asset or group of assets; (b,e) MWL relative to the ground floor
 481 of each asset; (c,f) ΔE , the elevation difference between the asset and the riverbed.

482 As concerns the correlation between LTV and MWL, Figure 5b highlights a clear relationship. Namely, the higher the
 483 flood depth, the greater the damage, as generally found in the literature for stage-damage functions. However, a lower



484 correlation is observed than the LTV-RS500 relationship as well as also a higher dispersion ($R^2=0.82$, $RMSE=0.17$). A
485 higher RMSE value can be justified by the Bellisio Solfare site, which represents an outlier. Indeed, the maximum
486 assigned LTV value due to its destruction is not solely linked to the MWL, but rather to the energy of the flow, as
487 demonstrated above.

488 The lowest correlation and the highest dispersion ($R^2=0.15$, $RMSE=0.21$) correspond to the LTV- ΔE relationship (Figure
489 5c).

490 Overall, the following results are worth highlighting:

- 491 • The correlation between LTV and *LIV* with ΔE is not statistically significant (p -value > 0.05).
- 492 • LTV and *LIV* are highly correlated (Pearson's $R=0.93$ and p -value < 0.05). Despite *LIV* considering factors not
493 directly related to the physical characteristics of a flood event, it still correlates well with LTV. Indeed, aesthetic
494 and communal value losses are generally sensitive to flood impacts, while evidential and historical values persist
495 despite flood damage, as the asset remains a testament to historical eras and past activities. However, if the asset
496 is destroyed, also intangible values are lost.
- 497 • RS (i.e., a proxy for river flow velocity) is highly correlated with LTV and *LIV* (Pearson's $R=0.85$ and 0.84 ,
498 respectively, and p -value < 0.05) but not significantly correlated with MWL (Pearson's $R=0.62$ and p -value $>$
499 0.05). Therefore, both RS and MWL are crucial for accurately estimating damage.

500 As mentioned in Sect. 2.2.4, also intrinsic factors can potentially influence the damages to CH. The presence of valuable
501 contents, especially if exposed at a low level with respect to the ground floor, increases the amount of damage, and then
502 the restoration cost. Indeed, the religious architectures that contain paintings, precious pews, and ancient elements such
503 as organs, have incurred in moderate or severe LTV, specifically the churches of S. Maria delle Tinte, S. Giovanni Battista,
504 and S. Nicolò (Table 4). On the other hand, although the S. Agostino and S. Maria del Porto churches contain artworks,
505 they have not experienced a loss in tangible value. This is attributed to their elevated positioning above ground floor level.
506 However, it could be noteworthy that their low LTV can also be attributed to their relatively low MWL (Table 4). A more
507 explanatory perspective on the positive impact of elevation on damage is the S. Nicolò church. Indeed, in this case, despite
508 a high MWL, the associated LTV is relatively low, as it is supra-elevated at 1.12 m above ground floor level (Table 4).
509 Even the state of conservation could influence the degree of damage. Indeed, the poor state of conservation reduced the
510 Bellisio Solfare asset capacity to resist the impact of the water and debris mixture, contributing to its destruction. This
511 data confirms that the degree of conservation can directly impact the extent of damage observed following a flood event
512 (Stephenson and D'Ayala, 2014; Salazar et al., 2024).

513 Studies in literature pinpoint the role of construction material in determining the vulnerability of CH assets (Balasbaneh
514 et al., 2020; Brokerhof et al., 2023). However, no relations were found for this parameter, as all the surveyed assets are
515 characterized by the same material (i.e., masonry structure). The only exception is the Ponte Garibaldi, which was
516 constructed with a reinforced concrete structure.

517 Among the factors that have contributed significantly to the overflowing of rivers during the 2022 Marche flood event
518 are bridges and culverts, which were clogged. In Cantiano, the inadequacy of the culverted section at the entrance of the
519 urban area resulted in insufficient drainage of the Burano River, leading to overflow and sediment deposition. In Pergola,
520 a bridge near the S. Maria delle Tinte church was blocked by sediment and woody debris, resulting in flooding of the
521 surrounding area. In Senigallia, large woody debris blocked Ponte Garibaldi, causing the flooding of the city. It is widely
522 observed that bridges and culverts can become clogged during intense bed load transport, hyper-concentrated flow, or
523 debris flow events, leading to massive overflows. To mitigate the risk of clogging in complex urban environments, a river
524 management approach that incorporates optimized design principles based on adequate field surveys, numerical



525 modelling, and laboratory experiments is desirable (Gschnitzer et al., 2017; Amaddii et al., 2022, 2023; Martín-Vide et
526 al., 2023; Zugliani et al., 2023). These measures would also positively impact the preservation of ancient CH assets, which
527 are now confronted with heightened flood risks due to climate change, a risk likely lower during their construction.

528 **4.2 Comparison between ex-post and ex-ante damage assessment**

529 In this section, the results obtained through the methodology outlined in Sect. 2.1 are presented and compared to the
530 results of the ex-post damage assessment, considering only the LTV.

531 The first issue with the flood hazard map is its low degree of detail. Indeed, all the areas investigated are in the same
532 class, namely “medium probability (low-frequency floods)”, and the map lacks some useful information, such as water
533 height or velocity. Thus, assets can only be included or excluded from floodable areas. Overlapping the assets of the MIC
534 database with the official map of flood hazard areas, 55 potentially damaged assets were identified. These assets were
535 then categorized based on their typology into various damage classes: 41 are included at risk of very high damage, 6 as
536 high, 5 as medium, and 2 as low. One of the individuated assets (“Fiorentino Basso”) remains unclassified due to
537 insufficient information available in the MIC database regarding its type. Additionally, the MIC database lacks
538 information regarding the type of value associated with each asset. It is noteworthy that only 5 in 55 identified assets are
539 listed as damaged cultural heritage in Table 4. Indeed, 37 cultural assets are residential, productive, rural, or tertiary
540 architectures, with no local or touristic/cultural interest. Moreover, some religious architectures or historical
541 infrastructures that are located in flood hazard areas were not damaged by the flood during the 15-16 September 2022
542 event.

543 In addition, it should be emphasized that 9 assets defy the ex-ante damage assessment, even if identified as damaged
544 during the field survey. This discrepancy arises either from their absence in the MIC database (such as Ponte Garibaldi,
545 S. Emidio oratory, and S. Maria del Porto church) or because they do not overlap with the flood hazard areas (including
546 Portici Ercolani, Bellisio Solfare refinery, Filanda Serica, historical buildings Via Fiorucci, S. Agostino church, and S.
547 Nicolò church).

548 These findings highlight the main issues with the MIC database:

- 549 ● Some assets may be inaccurately located (e.g., Bellisio Solfare refinery).
- 550 ● In cases where assets have an extended area and only a small portion is potentially inundated, the point shapefile
551 may not accurately represent their exposure, as it could be situated in unexposed areas (as observed with the
552 historical buildings Via Fiorucci and S. Agostino church). In the case of widespread assets or constructions with
553 a linear footprint (i.e., assets including several buildings along a road, or porches such as Portici Ercolani) only
554 one centroid point representative of the location exists.

555 Consequently, the comparison between the ex-ante and the ex-post damage assessments is feasible only for five assets:
556 Porta Lambertina, Ponte Grosso, Foro Annonario, S. Giovanni Collegiate, and S. Maria delle Tinte church. Consistently
557 with observations, from the ex-ante damage assessment it derives that the two churches fall in a very high damage class,
558 the Ponte Grosso bridge falls in a medium damage class, and the open space Foro Annonario falls in a low damage
559 class. Observed losses thus confirm that religious architectures are the most vulnerable to flooding as assumed in most of
560 the ex-ante flood risk assessment works in literature (Garrote et al., 2020; Arrighi et al., 2023). Concerning Porta
561 Lambertina, it resulted in a high damage class, while the ex-post assessment resulted in being slightly damaged, as only
562 mud marks were observed.



563 **5. Conclusions**

564 This paper developed an ex-post flood damage assessment method for CH assets. This yields a semi-quantitative on-site
565 evaluation of losses (i.e., not in monetary terms), both in terms of intangible and tangible impacts, that based on the best
566 of our knowledge constitutes a novel aspect. The method consists of four main steps: (i) identifying CH assets potentially
567 damaged by the flood; (ii) collecting post-event field data, through an ad-hoc developed survey form; (iii) evaluating the
568 losses in both intangible and tangible values; and (iv) analyzing the factors contributing to flood damage. For step (ii), it
569 is crucial to visit the damaged sites as soon as possible to collect data and information that may become unavailable due
570 to restoration work. The use of the proposed form allows a quick easy, and reproducible way for the post-event flood data
571 evaluation aimed at the direct assessment of losses in intangible and tangible values to CH assets. Then, step (iii) allows
572 us to estimate the level of losses caused by floods on both tangible and intangible values to different types of CH assets.
573 Finally, the findings from step (iv) allow for a better understanding of the causative phenomena aimed at valuable insights
574 for disaster risk management.

575 The method was applied to the CH assets damaged by the flood event that occurred on September 15-16 in the Burano,
576 Cesano, and Misa basins (Marche Region, Italy). The main findings that can be drawn from the application of the proposed
577 method are the following:

- 578 • Post-event field survey is fundamental for gathering data and information on the hazard characteristics, such as
579 water depths, together with losses in intangible and tangible values and for subsequent analysis (e.g., GIS
580 processing). Ex-post flood damage information for CH is relevant for verifying the hypothesis of existing
581 methods based on expert judgement. Moreover, it poses the basis for developing empirical flood vulnerability
582 functions for CH. Peculiarities of CH, such as raised floors, presence of valuable artworks, and state of
583 conservation are found to be relevant for flood vulnerability. Thus, where this information is not available, on-
584 site inspections are suggested to better characterize actual exposure and vulnerability for ex-ante risk analysis.
- 585 • The LTV is well correlated with the MWL, consistently with damages to other building types. Additionally,
586 there is also a strong correlation between LTV and the average slope of the riverbed, considering both 500 m
587 and 1000 m upstream of the assets. The slope of the riverbed, a proxy of river flow velocity, can thus be
588 considered as one of the possible contributing damage factors (as the measured or estimated data of water
589 velocity is difficult to obtain).
- 590 • The *LIV* correlates well to the same contributing factors, however, *LIV* data show a lower R^2 and a larger spread
591 demonstrating that intangible aspects are less dependent on flood characteristics. Nevertheless, LTV and *LIV*
592 are highly correlated, since some intangible values, e.g., aesthetic and communal values are sensitive to physical
593 flood damage, e.g., lack of accessibility.
- 594 • RS (i.e., a proxy for river flow velocity) is highly correlated with LTV and *LIV* but not significantly correlated
595 with MWL, and therefore, both RS and MWL are crucial for accurately estimating damage.

596 However, the method also presents some limitations:

- 597 • The baseline pre-disaster intangible value is obtained by combining four different typologies of value (aesthetic,
598 historical, evidential, communal) making some assumptions to identify the criteria for assigning the level of
599 value to each intangible aspect. Additional or alternative aspects, not currently accounted for, could influence
600 the assignment of intangible value.
- 601 • The limited number of surveyed assets does not allow for statistically robust relationships with contributing
602 factors. Indeed, other potential contributing factors could affect the observed damage (e.g., construction
603 material).



604 The existing exposure and vulnerability models, such as those by Arrighi et al. (2023), provide reasonable initial
605 predictions of potential damage to cultural heritage (CH). However, it should be emphasized that the available exposure
606 data are incomplete and inadequate for identifying all the flood-exposed assets and their vulnerability, leading to
607 inaccurate ex-ante damage assessments to CH, specifically:

- 608 • In the Burano, Cesano, and Misa basins, the official flood hazard map lacks the necessary detail to distinguish
609 which assets may suffer low or high flood damage, as it does not provide information on flood magnitude, such
610 as water depth and velocity.
- 611 • The MIC database includes immovable and movable assets encompassing those currently under protection, and
612 also those under verification. Therefore, an on-site direct check, conducted in collaboration with local
613 authorities, is always necessary to determine whether an asset qualifies as cultural heritage. Furthermore, the
614 database does not offer any information to delineate the value of assets, and in some cases, they are not
615 accurately geo-localized.

616 This paper underscores the importance of post-flood data collection and analysis. The proposed method serves as a starting
617 point for such data collection. Nevertheless, future research should include diverse cultural and geographic contexts to
618 improve accuracy, as the contributing factors can differently influence the observed damage. An open-source,
619 comprehensive CH database documenting flood-related damages, asset features (e.g., construction type, and building
620 material), and factors describing the event magnitude (e.g., maximum water level) is needed. Additionally, quantifying
621 tangible damage in monetary terms should allow us to obtain a more robust evaluation of the damage to CH assets.
622 Nonetheless, it requires collaboration with government institutions to share monetary data (e.g., restoration costs). These
623 steps would enhance flood risk management for CH conservation and help develop robust damage prediction models.

624 *Data availability.* GIS data and ex-post damage survey form will be made available in a public repository after acceptance.

625 *Author contributions.* CA conceptualized the research idea; CA and CDL equally contributed to the planning of the on-
626 site data collection and performed the measurements; CA, CDL, and MA developed the methodology; MA, CDL, and
627 CA analyzed the data; MA performed GIS analysis; MA handled the data visualization; CA supervised the research
628 activity; MA and CDL wrote the manuscript draft; CA reviewed and edited the manuscript.

629 *Competing interests.* The authors declare that they have no conflict of interest.

630 *Acknowledgements.* The authors express their gratitude to the working group “MARCHE 2022”
631 (<https://sites.google.com/view/misa2022/home-page>) for their collaboration in the post-event data collection phase.

632 *Financial support.* This study was carried out within the RETURN Extended Partnership and received funding from the
633 European Union Next-Generation EU (National Recovery and Resilience Plan – NRRP, Mission 4, Component 2,
634 Investment 1.3 – D.D. 1243 2/8/2022, PE0000005).

635 **References**



- 636 Adeyemo, O.J., Maksimovic, C., Booyan –Aaronnet, S., Leitao, J., Butler, D., Makropoulos, C., 2008. Sensitivity analysis
637 of surface runoff generation for Pluvial Urban Flooding. In: 11th International Conference on Urban Drainage, Edinburgh,
638 Scotland, UK, 2008.
- 639 Al-Kindi, K.M. and Alabri, Z. Investigating the Role of the Key Conditioning Factors in Flood Susceptibility Mapping
640 Through Machine Learning Approaches. *Earth Syst Environ* 8, 63–81 (2024). [https://doi.org/10.1007/s41748-023-00369-](https://doi.org/10.1007/s41748-023-00369-7)
641 [7](https://doi.org/10.1007/s41748-023-00369-7).
- 642 Alexandrakis, G.; Manasakis, C.; Kampanis, N.A. Economic and Societal Impacts on Cultural Heritage Sites, Resulting
643 from Natural Effects and Climate Change. *Heritage* 2019, 2, 279-305. <https://doi.org/10.3390/heritage2010019>.
- 644 Amaddii, M.; Rosatti, G.; Zugliani, D.; Marzini, L.; Disperati, L. Back-Analysis of the Abbadia San Salvatore (Mt.
645 Amiata, Italy) Debris Flow of 27–28 July 2019: An Integrated Multidisciplinary Approach to a Challenging Case Study.
646 *Geosciences* 2022, 12, 385. <https://doi.org/10.3390/geosciences12100385>.
- 647 Amaddii M., Rosatti G., Zugliani D., Marzini L. & Disperati L. (2023) - Modelling stony debris flows involving culverted
648 streams: the Abbadia San Salvatore case (Mt. Amiata, Italy). *Rend. Online Soc. Geol.It.*, 61, 108-115,
649 <https://doi.org/10.3301/ROL.2023.55>.
- 650 Anderson, K. The impact of increased flooding caused by climate change on heritage in England and North Wales, and
651 possible preventative measures: what could/should be done?. *Built Heritage* 7, 7 (2023). [https://doi.org/10.1186/s43238-](https://doi.org/10.1186/s43238-023-00087-z)
652 [023-00087-z](https://doi.org/10.1186/s43238-023-00087-z).
- 653 ANSA, Regione Marche: [https://www.ansa.it/marche/notizie/2023/11/07/senigalliademolito-ponte-garibaldi-simbolo-](https://www.ansa.it/marche/notizie/2023/11/07/senigalliademolito-ponte-garibaldi-simbolo-dellalluvione-2022_c834fc28-e7c4-4e8d-9573-0346a0c13560.html)
654 [dellalluvione-2022_c834fc28-e7c4-4e8d-9573-0346a0c13560.html](https://www.ansa.it/marche/notizie/2023/11/07/senigalliademolito-ponte-garibaldi-simbolo-dellalluvione-2022_c834fc28-e7c4-4e8d-9573-0346a0c13560.html), last access: 27 May 2024 (2023).
- 655 Arrighi, C.; Brugioni, M.; Castelli, F.; Franceschini, S.; Mazzanti, B. Flood risk assessment in art cities: the exemplary
656 case of Florence (Italy). *J. Flood Risk Manage.* (2018), S616, <https://doi.org/10.1111/jfr3.12226>, 31.
- 657 Arrighi, C. A global scale analysis of river flood risk of UNESCO world heritage sites, *Frontiers in Water* 3 (2021) 1–12,
658 <https://doi.org/10.3389/frwa.2021.764459>. December.
- 659 Arrighi, C.; Carraresi A.; Castelli, F. Resilience of art cities to flood risk: a quantitative model based on depth-idleness
660 correlation, *J. Flood Risk Manage.* 15 (2) (2022) 1–15, <https://doi.org/10.1111/jfr3.12794>.
- 661 Arrighi, C.; Tanganelli, M.; Cristofaro, M.T. et al. Multi-risk assessment in a historical city. *Nat Hazards* 119, 1041–1072
662 (2023a). <https://doi.org/10.1007/s11069-021-05125-6>.
- 663 Arrighi, C.; Ballio, F.; Simonelli, T. 2023b. A GIS-based flood damage index for cultural heritage. *International Journal*
664 *of Disaster Risk Reduction* 90, 103654. <https://doi.org/10.1016/j.ijdr.2023.103654>.
- 665 AUBAC: <https://webgis.abdac.it/portal/apps/webappviewer/index.html?id=b4f5f37d97e9427c9c2e4ce7e30928f9>, last
666 access: 27 May 2024.
- 667 Balasbaneh, A.T. et al 2020 IOP Conf. Ser.: Earth Environ. Sci. 476 012004 DOI 10.1088/1755-1315/476/1/012004.
- 668 Beven, K.J. and Kirby, M.J. 1979. A physically based variable contributing area model of basin hydrology. *Hydrological*
669 *Science Bulletin* 24, 43–69.
- 670 Brokerhof, A.W.; van Leijen, R.; Gersonius, B. Protecting Built Heritage against Flood: Mapping Value Density on Flood
671 Hazard Maps. *Water* 2023, 15, 2950. <https://doi.org/10.3390/w15162950>.
- 672 Clini, P.; Muñoz-Cádiz, J.; Ferretti, U.; Jiménez, J.L.D. Nieto, G.M. (2023). Digital Transition for Heritage Management
673 and Dissemination: via Flaminia and Corduba-Emerita. In Cannella M., Garozzo A., Morena S. (Eds.). *Transizioni. Atti*
674 *del 44° Convegno Internazionale dei Docenti delle Discipline della Rappresentazione/Transitions. Proceedings of the*
675 *44th International Conference of Representation Disciplines Teachers. Milano: FrancoAngeli, pp. 2613-2622.*



- 676 COPERNICUS Emergency Management Service: [https://emergency.copernicus.eu/mapping/list-of-](https://emergency.copernicus.eu/mapping/list-of-components/EMSR634)
677 [components/EMSR634](https://emergency.copernicus.eu/mapping/list-of-components/EMSR634), last access: 27 May 2024 (2022).
- 678 CRED (2015). The Human Cost of Natural Disasters 2015: A Global Perspective. Retrieved from:
679 https://reliefweb.int/sites/reliefweb.int/files/resources/PAND_report. (accessed April 18, 2024).
- 680 Cuca, B. and Barazzetti, L.: Damages from extreme flooding events to cultural heritage and landscapes: water component
681 estimation for Centa River (Albenga, Italy), *Adv. Geosci.*, 45, 389–395, <https://doi.org/10.5194/adgeo-45-389-2018>,
682 2018.
- 683 D.lgs. 22 gennaio 2004, n. 42: [https://www.normattiva.it/esporta/attoCompleto?atto.dataPubblicazioneGazzetta=2004-](https://www.normattiva.it/esporta/attoCompleto?atto.dataPubblicazioneGazzetta=2004-02-24&atto.codiceRedazionale=004G0066)
684 [02-24&atto.codiceRedazionale=004G0066](https://www.normattiva.it/esporta/attoCompleto?atto.dataPubblicazioneGazzetta=2004-02-24&atto.codiceRedazionale=004G0066), last access: 27 May 2024 (2004).
- 685 Dall’Osso, F.; Gonella, M.; Gabbianelli, G.; Withycombe, G.; Dominey-Howes, D. (2009) A revised (PTVA) model for
686 assessing the vulnerability of buildings to tsunamis damage. *Nat Hazards Earth Syst Sci* 9:1557–1565.
- 687 De Donatis, M.; Lepore, G.; Susini, S.; Silani, M.; Boschi, F.; Savelli, D. Sistemi informativi geografici e modellazione
688 tridimensionale per la Geo-archeologia a Senigallia: Nuove scoperte e nuove ipotesi. *Rend. Online Soc. Geol. Ital.* 2012,
689 19, 16–19.
- 690 De Donatis, M.; Nesci, O.; Savelli, D.; Pappafico, G.F.; Susini, S. Geomorphological Evolution of the Sena Gallica Site
691 in the Morpho-Evolutive Quaternary Context of the Northern-Marche Coastal Sector (Italy). *Geosciences* 2019, 9, 272.
692 <https://doi.org/10.3390/geosciences9060272>.
- 693 Deschaux, J. 4 - Flood-related Impacts on Cultural Heritage, Editor(s): Freddy Vinet, *Floods*, Elsevier, 2017, Pages 53-
694 72, ISBN 9781785482687, <https://doi.org/10.1016/B978-1-78548-268-7.50004-3>.
- 695 Di Salvo, C.; Pennica, F.; Ciotoli, G.; Cavinato, G.P. A GIS-based procedure for preliminary mapping of pluvial flood
696 risk at metropolitan scale, *Environmental Modelling & Software*, Volume 107, 2018, Pages 64-84, ISSN 1364-8152,
697 <https://doi.org/10.1016/j.envsoft.2018.05.020>.
- 698 Dottori, F., Mentaschi, L., Bianchi, A. et al. Cost-effective adaptation strategies to rising river flood risk in Europe. *Nat.*
699 *Clim. Chang.* 13, 196–202 (2023). <https://doi.org/10.1038/s41558-022-01540-0>.
- 700 Drdácáký, M.F. Impact of Floods on Heritage Structures. *J. Perform. Constr. Facil.* 2010, 24, 430–431.
- 701 Dutta D, Wright W, Rayment P (2011) Synthetic impact response functions for flood vulnerability analysis and adaptation
702 measures in coastal zones under changing climatic conditions: a case study in Gippsland coastal region, Australia. *Nat*
703 *Hazards* 59(2):967–986. <https://doi.org/10.1007/s11069-011-9812-x>.
- 704 ESRI. ArcGIS PRO: release 3.2.2. Redlands, CA: Environmental Systems Research Institute; 2023.
- 705 EU. Directive 2007/60/EC of the European Parliament and of the Council of 23 October 2007 on the Assessment and
706 Management of Flood Risks; European Environment Agency: Copenhagen, Denmark, 2007; pp. 27–34.
- 707 Fatorić, S., & Seekamp, E. (2017). Are cultural heritage and resources threatened by climate change? A systematic
708 literature review. *Climatic Change*, 142(1–2), 227–254. <https://doi.org/10.1007/s10584-017-1929-9>.
- 709 Figueiredo, R.; Romão, X.; Paupério, E. Flood risk assessment of cultural heritage at large spatial scales: Framework and
710 application to mainland Portugal, *Journal of Cultural Heritage*, Volume 43, 2020, Pages 163-174, ISSN 1296-2074,
711 <https://doi.org/10.1016/j.culher.2019.11.007>.
- 712 Figueiredo, R., Romao, X., & Paupério, E. (2021). Component-based flood vulnerability modelling for cultural heritage
713 buildings. *International Journal of Disaster Risk Reduction*, 61(January), 102323.
714 <https://doi.org/10.1016/j.ijdrr.2021.102323>.



- 715 Galasso, C., Pregolato, P., Parisi, F. A model taxonomy for flood fragility and vulnerability assessment of buildings,
716 International Journal of Disaster Risk Reduction, Volume 53, 2021, 101985, ISSN 2212-4209,
717 <https://doi.org/10.1016/j.ijdr.2020.101985>.
- 718 Garrote, J.; Gutiérrez-Pérez, I.; Díez-Herrero, A. Can the quality of the potential flood risk maps be evaluated? A case
719 study of the social risks of floods in Central Spain. *Water* 2019, 11, 1284.
- 720 Garrote, J., A. Díez-Herrero, C. Escudero, and I. Garcia. 2020. A framework proposal for regional-scale flood-risk
721 assessment of cultural heritage sites and application to the Castile and León region (central Spain). *Water* 12(2): Article
722 329.
- 723 GLI ANGELI DELLE TINTE: <https://fondoambiente.it/il-fai/grandi-campagne/i-luoghi-del-cuore/comitati/1347>, last
724 access: 27 May 2024 (2022).
- 725 Godfrey, A.; Ciurean, R.L.; Van Westen, C.J.; Kingma, N.C.; Glade, T. Assessing Vulnerability of Buildings to Hydro-
726 Meteorological Hazards Using an Expert Based Approach—An Application in Nehoiu Valley, Romania. *Int. J. Disaster*
727 *Risk Reduct.* 2015, 13, 229–241.
- 728 Gschnitzer, T.; Gems, B.; Mazzorana B.; Aufleger M. Towards a robust assessment of bridge clogging processes in flood
729 risk management, *Geomorphology*, Volume 279, 2017, Pages 128-140, ISSN 0169-555X,
730 <https://doi.org/10.1016/j.geomorph.2016.11.002>.
- 731 HE. 2008. Conservation principles - policies and guidance for the sustainable management of the historic environment.
732 London: Historic England.
- 733 Huijbregts, Z., van Schijndel, J. W. M., Schellen, H. L., & Blades, N. (2014). Hygrothermal modelling of flooding events
734 within historic buildings. *Journal of Building Physics*, 38(2), 170–187. <https://doi.org/10.1177/1744259114532613>.
- 735 Iacobucci, G.; Piacentini, D.; Troiani, F. Enhancing the Identification and Mapping of Fluvial Terraces Combining
736 Geomorphological Field Survey with Land-Surface Quantitative Analysis. *Geosciences* 2022, 12, 425.
737 <https://doi.org/10.3390/geosciences12110425>.
- 738 IPCC. 2023: Sections. In *Climate Change 2023: Synthesis Report; Contribution of Working Groups I, II and III to the*
739 *Sixth Assessment Report of the Intergovernmental Panel on Climate Change; Core Writing Team, Lee, H., Romero, J.,*
740 *Eds.; IPCC: Geneva, Switzerland, 2023; pp. 35–115.*
- 741 Istituto Superiore per la Conservazione ed il Restauro – MiBACT:
742 <http://vincoliinrete.beniculturali.it/VincoliInRete/vir/bene/listabeni>, last access: 27 May 2024.
- 743 Jeggle, T. and Boggero, M. (2018). Post-Disaster Needs Assessment (PDNA): Lessons from a Decade of Experience
744 (English). Washington, D.C.: World Bank Group.
745 [http://documents.worldbank.org/curated/en/481761539848031116/Post-Disaster-Needs-Assessment-PDNA-Lessons-](http://documents.worldbank.org/curated/en/481761539848031116/Post-Disaster-Needs-Assessment-PDNA-Lessons-from-a-Decade-of-Experience)
746 [from-a-Decade-of-Experience](http://documents.worldbank.org/curated/en/481761539848031116/Post-Disaster-Needs-Assessment-PDNA-Lessons-from-a-Decade-of-Experience).
- 747 Kefi, M., Mishra, B.K., Masago, Y. et al. Analysis of flood damage and influencing factors in urban catchments: case
748 studies in Manila, Philippines, and Jakarta, Indonesia. *Nat Hazards* 104, 2461–2487 (2020).
749 <https://doi.org/10.1007/s11069-020-04281-5>.
- 750 Kreibich, H. and Thieken, A.H. (2008) Assessment of damage caused by high groundwater inundation. *Water Resour*
751 *Res* 44:W09409. <https://doi.org/10.1029/2007W R0066 21>.
- 752 Marín-García, D.; Rubio-Gómez-Torga, J.; Duarte-Pinheiro, M.; Moyano, J. Simplified automatic prediction of the level
753 of damage to similar buildings affected by river flood in a specific area, *Sustainable Cities and Society*, Volume 88, 2023,
754 104251, ISSN 2210-6707, <https://doi.org/10.1016/j.scs.2022.104251>.



- 755 Mark, O., Weesakul, S., Apirumanekul, C., Boonya Aroonet, S., Djordjevic, S., 2004. Potential and limitations of 1D
756 modelling of urban flooding. *J. Hydrol.* 299, 284–299. <http://dx.doi.org/10.1016/j.jhydrol.2004.08.014>.
- 757 Martín-Vide, J.P.; Bateman A.; Berenguer M.; Ferrer-Boix C.; Amengual A.; Campillo M.; Corral C.; Llasat M.C.; Llasat-
758 Botija M.; Gómez-Dueñas S.; Marín-Esteve B.; Núñez-González F.; Prats-Puntí A.; Ruiz-Carulla R.; Sosa-Pérez R. Large
759 wood debris that clogged bridges followed by a sudden release. The 2019 flash flood in Catalonia., *Journal of Hydrology:
760 Regional Studies*, Volume 47, 2023, 101348, ISSN 2214-5818, <https://doi.org/10.1016/j.ejrh.2023.101348>.
- 761 Marzeion, B., & Levermann, A. (2014). Loss of cultural world heritage and currently inhabited places to sea-level rise.
762 *Environmental Research Letters*, 9(3), 034001. <https://doi.org/10.1088/1748-9326/9/3/034001>.
- 763 MASE, Geoportale Nazionale: <https://gn.mase.gov.it/portale/distribuzione-dati-pst> , last access 27 May 2024.
- 764 Mastrorillo, L. and Petitta, M. (2014). Effective infiltration variability in the Umbria-Marche carbonate aquifers of central
765 Italy. *Journal of Mediterranean Earth Sciences*, 2. <https://doi.org/10.3304/JMES.2010.004>.
- 766 Merz, B., Blöschl, G., Vorogushyn, S., Dottori, F., Aerts, J. C. J. H., Bates, P., et al. (2021). Causes, impacts and patterns
767 of disastrous river floods. *Nat. Rev. Earth Environ.* 2, 592–609. doi: 10.1038/s43017-021-00195-3.
- 768 Molinari, D., Menoni, S., Aronica, G. T., Ballio, F., Berni, N., Pandolfo, C., Stelluti, M., and Minucci, G.: Ex post damage
769 assessment: an Italian experience, *Nat. Hazards Earth Syst. Sci.*, 14, 901–916, doi:10.5194/nhess-14-901-2014, 2014.
- 770 Momčilović Petronijević, A.; Petronijević, P. Floods and Their Impact on Cultural Heritage—A Case Study of Southern
771 and Eastern Serbia. *Sustainability* 2022, 14, 14680. <https://doi.org/10.3390/su142214680>.
- 772 Moore, P.D., Webb, J.A.; Collinson M.E. (1991) Pollen analysis. Blackwell Scientific, Oxford.
- 773 Pulvirenti, L.; Squicciarino, G.; Fiori, E.; Candela, L.; Puca, S. Analysis and Processing of the COSMO-SkyMed Second
774 Generation Images of the 2022 Marche (Central Italy) Flood. *Water* 2023, 15, 1353. <https://doi.org/10.3390/w15071353>.
- 775 Ravan, M., Revez, M.J., Pinto, I.V. et al. A Vulnerability Assessment Framework for Cultural Heritage Sites: The Case
776 of the Roman Ruins of Tróia. *Int J Disaster Risk Sci* 14, 26–40 (2023). <https://doi.org/10.1007/s13753-023-00463-4>.
- 777 REGIONE MARCHE, ANNALI IDROLOGICI:
778 https://www.regione.marche.it/portals/0/Protezione_Civile/Manuali%20e%20Studi/annale-parte-I-2021.pdf, last access:
779 27 May 2024 (2021).
- 780 REGIONE MARCHE, RAPPORTO DI EVENTO preliminare:
781 https://www.regione.marche.it/portals/0/Protezione_Civile/Manuali%20e%20Studi/Rapporto_Evento_preliminare_20220915.pdf, last access: 27 May 2024 (2022).
- 782
- 783 REGIONE MARCHE, Ambiente: [https://www.regione.marche.it/Regione-Utile/Paesaggio-Territorio-](https://www.regione.marche.it/Regione-Utile/Paesaggio-Territorio-Urbanistica/Cartografia)
784 [Urbanistica/Cartografia](https://www.regione.marche.it/Regione-Utile/Paesaggio-Territorio-Urbanistica/Cartografia), last access: 27 May 2024 (2023).
- 785 Reimann, L., Vafeidis, A. T., Brown, S., Hinkel, J., & Tol, R. S. J. (2018). Mediterranean UNESCO world heritage at
786 risk from coastal flooding and erosion due to sea-level rise. *Nature Communications*, 9(1), 4161.
787 <https://doi.org/10.1038/s41467-018-06645-9>.
- 788 Riley SJ, DeGloria SD, Elliot R (1999) A terrain ruggedness index that quantifies topographic heterogeneity. *Int J Sci*
789 5(1–4):23–27.
- 790 Romao, X., Paupério, E., Monserrat, O., Rousakis, T., & Montero, P. (2020). Assets at risk and potential impacts: 3.6 -
791 Cultural heritage. *Science for disaster risk management 2020: Acting Today, Protecting Tomorrow*, pp. 503–525.
- 792 Romão, X., & Paupério, E. (2021). An Indicator for Post-disaster Economic Loss Valuation of Impacts on Cultural
793 Heritage. *International Journal of Architectural Heritage*, 15(5), 678–697.
794 <https://doi.org/10.1080/15583058.2019.1643948>.



- 795 Sabbioni, C., Brimblecombe, P., Bonazza, A., Grossi, C. M., Harris, I., & Messina, P. Mapping climate change and
796 cultural heritage. In: M., D. & M., C. (eds.). *Safeguarding Cultural Heritage. Understanding & Viability for the Enlarged*
797 *Europe.*, 2006 Prague, Czech Republic.: Institute of Theoretical and Applied Mechanics of the Academy of Sciences of
798 the Czech Republic, 119–124.
- 799 Salazar, L.G.F., Romão, X., Figueiredo, R. (2024). A Hybrid Approach for the Assessment of Flood Vulnerability of
800 Historic Constructions and Their Contents. In: Endo, Y., Hanazato, T. (eds) *Structural Analysis of Historical*
801 *Constructions.* SAHC 2023. RILEM Bookseries, vol 46. Springer, Cham. https://doi.org/10.1007/978-3-031-39450-8_91.
- 802 Schlumberger, J., Ferrarin, C., Jonkman, S. N., Diaz Loaiza, M. A., Antonini, A., and Fatorić, S.: Developing a framework
803 for the assessment of current and future flood risk in Venice, Italy, *Nat. Hazards Earth Syst. Sci.*, 22, 2381–2400,
804 <https://doi.org/10.5194/nhess-22-2381-2022>, 2022.
- 805 Sesana E, Gagnon AS, Ciantelli C, Cassar JA, Hughes JJ. Climate change impacts on cultural heritage: A literature review.
806 *WIREs Clim Change.* 2021; 12:e710. <https://doi.org/10.1002/wcc.710>.
- 807 Shepard, D. A two-dimensional interpolation function for irregularly-spaced data. In *Proceedings of the 1968 23rd ACM*
808 *National Conference*, New York, NY, USA, 27–29 August 1968; pp. 517–524.
- 809 SIRMIP ON-LINE: <http://app.protezionecivile.marche.it/sol/indexjs.sol?lang=it>, last access: 27 May 2024.
- 810 Smith, D.I. (1994) Flood damage estimation—a review of urban stage-damage curves and loss functions. *Water SA*
811 20:231–238.
- 812 Stephenson, V. and D'Ayala, D.: A new approach to flood vulnerability assessment for historic buildings in England, *Nat.*
813 *Hazards Earth Syst. Sci.*, 14, 1035–1048, <https://doi.org/10.5194/nhess-14-1035-2014>, 2014.
- 814 Storm Chasers Marche: <https://www.youtube.com/watch?v=wNFpouu4aSg>, last access: 27 May 2023 (2022).
- 815 Sulphur, MARCHE MINING GEOPARK: <https://www.museumulphur.it/en/marche-mining-geopark/>, last access: 27
816 May 2024.
- 817 Tarquini S., I. Isola, M. Favalli, F. Mazzarini, M. Bisson, M.T. Pareschi, E. Boschi (2007). TINITALY/01: a new
818 triangular irregular network of Italy. *Annals of Geophysics.* <https://doi.org/10.4401/ag-4424>.
- 819 Tarquini S., I. Isola, M. Favalli, A. Battistini, G. Dotta (2023). TINITALY, a digital elevation model of Italy with a 10
820 meters cell size (Version 1.1). Istituto Nazionale di Geofisica e Vulcanologia (INGV).
821 <https://doi.org/10.13127/tinality/1.1>.
- 822 TGCOM24: [https://www.tgcom24.mediaset.it/2022/video/alluvione-marche-a-cantiano-il-ponte-romano-resiste-al-](https://www.tgcom24.mediaset.it/2022/video/alluvione-marche-a-cantiano-il-ponte-romano-resiste-al-disastro_55048806-02k.shtml)
823 [disastro_55048806-02k.shtml](https://www.tgcom24.mediaset.it/2022/video/alluvione-marche-a-cantiano-il-ponte-romano-resiste-al-disastro_55048806-02k.shtml), last access: 27 May 2024 (2022).
- 824 Trizio, F.; Torrijo, F.J.; Mileto, C.; Vegas, F. Flood Risk in a Heritage City: Alzira as a Case Study. *Water* 2021, 13,
825 1138. <https://doi.org/10.3390/w13091138>
- 826 Vafadari, A.; Philip, G.; Jennings, R. J. T. I. A. o. t. P., Remote Sensing; Sciences, S. I., Damage assessment and
827 monitoring of cultural heritage places in a disaster and post-disaster event—a case study of Syria. 2017, 42, 695-701.
- 828 Vecvagars, K. (2006). Valuing damage and losses in cultural assets after a disaster: Concept paper and research options
829 (CEPALSERI). United Nations Publication.
- 830 Wallemacq, P., Guha-Sapir, D., McClean, D., Cred, and Unisdr: *The Human Cost of Natural Disasters – A global*
831 *perspective*, United Nations Office for Disaster Risk Reduction (UNISDR), Geneva, Switzerland, 2015.
- 832 Wang, J.-J. (2015). Flood risk maps to cultural heritage: Measures and process. *Journal of Cultural Heritage*, 16(2), 210–
833 220. <https://doi.org/10.1016/j.culher.2014.03.002>.
- 834 Willis, K.G. The Use of Stated Preference Methods to Value Cultural Heritage (2014). *Handbook of the Economics of*
835 *Art and Culture*, 2, pp. 145-181. Cited 33 times.



- 836 http://www.elsevier.com/wps/find/bookdescription.cws_home/622130/description#description doi: 10.1016/B978-0-
837 444-53776-8.00007-6.
- 838 World Events News: <https://www.youtube.com/watch?v=HjOYO-GS0dM>, last access: 27 May 2024 (2022).
- 839 Zhang, S-N; Ruan, W-Q; Li, Y-Q; Xiao, H. Cultural distortion risks at heritage sites: Scale development and validation,
840 *Tourism Management*, Volume 102, 2024, 104860, ISSN 0261-5177, <https://doi.org/10.1016/j.tourman.2023.104860>.
- 841 Zugliani, D., Ataieyan, A., Rocco, R., Betemps, N., Ropele, P., Rosatti, G. Bridge obstruction caused by debris flow: A
842 practical procedure for its management in debris-flow simulations (Open Access) (2023) *E3S Web of Conferences*, 415,
843 art. no. 05031. [www.e3s-conferences.org/doi: 10.1051/e3sconf/202341505031](http://www.e3s-conferences.org/doi/10.1051/e3sconf/202341505031).